

NUMERICAL AND EXPERIMENTAL ANALYSIS OF HEAT TRANSFER IN MICROPROCESSOR HEAT SINK

Verônica de Liz Borges*, veriskilp@gmail.com

Carlos Alberto de Almeida Vilela*, carlosavgeo@yahoo.com

*Instituto Federal de Educação, Ciência e Tecnologia de Goiás (IF-Goiás)

Abstract

One of the major challenges in computer and electronic design is the electronic cooling. Knowing that electronics is always in evolution and increasing the computational speed, the power consumption is increasing as well. A considerable part of this consumed power is transformed into heat that must be dissipated otherwise serious problems can arise in the system. This paper presents a numerical and experimental comparative study of two different models of heat sink used in electronic cooling. The mean processor temperature were measured and compared to numerical results. Velocity and temperature distribution over the heat sink were evaluated using finite element software and the Nusselt number were evaluated using numerical and experimental values. The major objective of this paper is present a procedure to determine numerically or experimentally heat transfer parameters like Nusselt number and convective heat transfer coefficient to complex geometries.

Keywords: *electronic cooling, computational simulation, finite element, microprocessor, convective heat transfer*

1. INTRODUCTION

With the increasing computational power of each processor new generation, there is an increasing in electric power consumption as well and this leads to increasing heat generation inside the processor that must be dissipated somehow. As an example, let's remember some years ago when Intel released the 80286 processor model, that heat dissipation was about 0.8 – 1.0 W/cm². Today is usual to find in personal computers Core 2 processors model which heat dissipation is about 170 W/cm². This is a huge step in heat generation. In the same way, the processing speed jump from 6 - 25 MHz (80286 model) to 2.33 GHz (Core 2 model), and the number of transistors jump from 1.34x10⁵ to 2.91x10⁸. Table 1 presents the heat dissipation level referred to some Alpha processors models, and Fig. 1 presents the heat dissipation evolution to some Intel processors models.

Table 1. Power dissipations of Compaq Alpha processors. Wilcox, and Manne (1999).

Processor	Power [W]	Frequency [MHz]	Die Area [mm ²]	Voltage [V]
21064	30	200	234	3.3
21164	50	300	299	3.3
21264	90	575	313	2.2
21364	100	1000	340	1.5
21464	150	2000	396	1.2

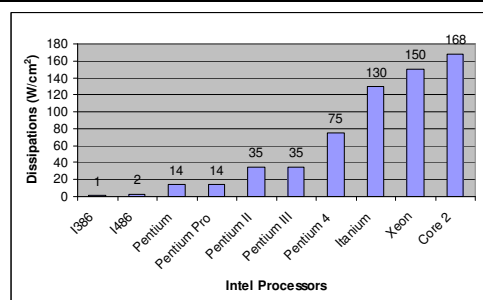


Figure 1. Intel processors power dissipations. Pollack (1999), Han (2007)

Considering that today microprocessors can reach about 170 W/cm^2 ($170 \times 10^4 \text{ W/m}^2$) of heat dissipation without over clocking and, to assure its performance, the maximum operational temperature is about $90 \text{ }^\circ\text{C}$, so there is a big challenge, that is dissipate all the generated heat in a small ambient and with low level noise.

In this work was considered as reference a Celeron 700 MHz Intel processor model, and some general characteristics is shown in Tab. 2, comparing to some others Intel models.

Table 2. Thermal specifications for Intel Pentium processors, Intel Corporation^[1](2002)

Core Frequency [MHz]	L2 Cache Size [Kbytes]	Thermal Design Power [W]	L2 Cache Power [W]	Power Density [W/cm^2]	Max T [$^\circ\text{C}$]
Pentium 500	512	28.0	1.33	23.9	90
Pentium 600	512	34.5	1.60	29.5	85
Pentium 700	256	18.3	NA	25.2	80
Pentium 800	256	20.8	NA	28.7	80
Celeron 700	128	19.1	NA	21.9	80

Intel recommends that to assure the processor perfect performance, the maximum core temperature permitted is $80 \text{ }^\circ\text{C}$, considering Celeron 700 model. In this microprocessor most of the heat is generated inside the Core area and a small portion of heat is generated inside L2 Cache area, described in Fig. 2a.

This leads Intel to add an extended heat dissipation plate over the Core area, and the recommendation is that only the heat passing through this plate should be externally helped dissipated by heat sink and coolers. A typical example of microprocessor / heat sink assembly, just like the model used in this work, is shown in Fig 2b, that shows the ambient and case temperature measuring point. The case temperature is considered as the maximum allowed operation temperature by Intel, and for this reason this will be monitored.

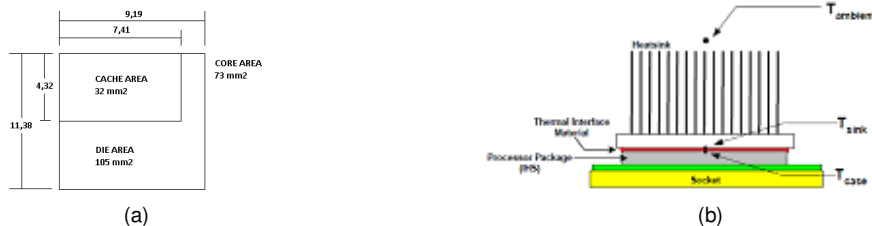


Figure 2. (a) Intel processor die layout, (b) heat sink assembly and temperature measuring points. Intel Corporation^[1](2002)

The importance of controlling heat dissipation is due the fact that if the microprocessor temperature goes higher than the maximum allowed by Intel, it becomes instable and surely will have a breakdown. Pecht *et al* (1992) says that these fails happens because of heat tensions, chemical reactions and dielectric break, and the temperature rising of 10 to $20 \text{ }^\circ\text{C}$ by over clocking or cooler low performance can duplicate the fail occurrence, Bejan, Jones and Krauss (2003). Toshiba scientists reach an increasing of 37% in processing performance keeping the microprocessor temperature at $-33 \text{ }^\circ\text{C}$. It is equivalent to shrink a generation jump. Also some significant results were obtained keeping the microprocessor at room temperature, about $27 \text{ }^\circ\text{C}$. At this temperature level it is possible to reach until 19% increasing performance. Each $10 \text{ }^\circ\text{C}$ colder you have a 5% boost in performance, Technology News (2007)

2. EXPERIMENTAL APPARATUS

This work proposal is to study the heat transfer and air flow pattern in a microprocessor / heat sink assembly used in personal computers. To proceed to this analysis, an experimental apparatus was built to experimental data acquisition and also was used a computational tool to simulate several cases with several boundary conditions and materials. A description of experimental apparatus with microprocessor general dimensions considered in this study is shown in Fig 3. This experimental apparatus was composed by an air flow tunnel used to air direction, a control valve and an orifice plate to air flow measuring. The air is driven by a blower fixed over the heat sink that is fixed over the microprocessor heat dissipation plate.

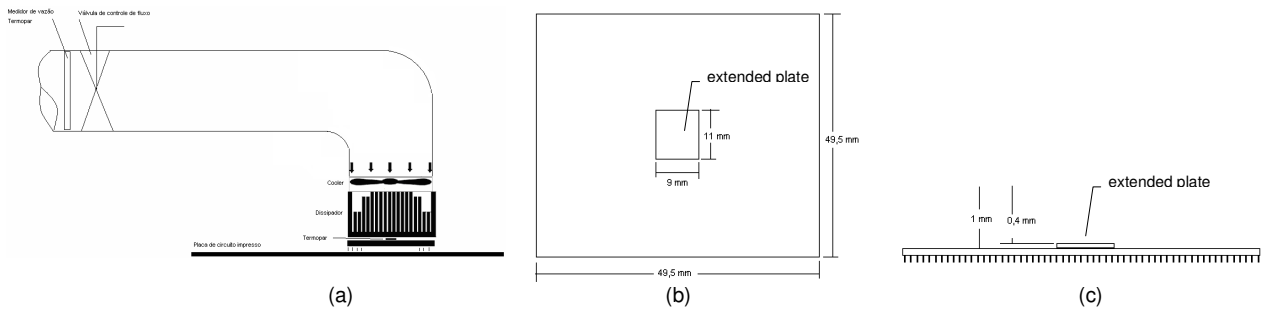


Figure 3. (a) Experimental apparatus scheme, (b), (c) processor general dimensions.

The heat sink models used in this study are shown in Fig 4. The computational models, called as solid domain, and part of the fluid domain, the air domain, are also shown.

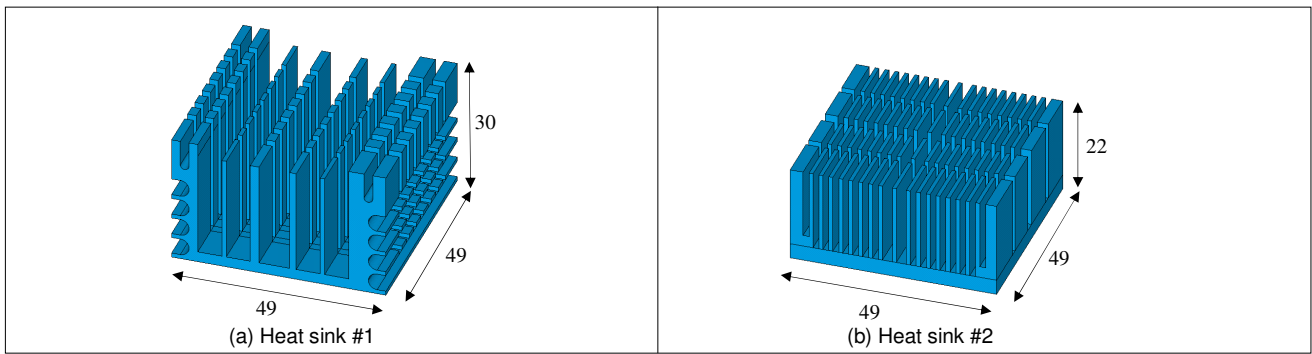


Figure 4. Heat sink general dimensions. (a) model #1, (b) model #2. Dimensions in millimeters.

The thermo-physical properties of air and heat sink materials, copper and aluminum, are listed in Tab. 3.

Table 3. Thermo physical properties for materials.

	Density [kg/m ³]	Specific Heat [J/kg.°C]	Dynamic Viscosity [Pa.s]	Thermal Conductivity [W/m.°C]	Thermal Diffusivity [m ² /s]	Prandtl
Air (25 °C)	1.1774	100.57	18.462e-6	0.02624	2.29e-5	0.7
Aluminum	2707.0	896.0	-	220.0	97.1e-6	-
Copper	8933.0	385.0	-	401.0	117e-6	-

3. GOVERNING EQUATIONS AND BOUNDARY CONDITIONS

Were considered two distinct configurations for numerical simulation: first considering the case without heat sink and second considering the case with heat sink. For without heat sink cases, were considered a transient two-dimensional solution with a computational domain boundary passing through the symmetry plane along the vertical axes through the center of the microprocessor, and for with heat sink cases were considered a tri-dimensional steady state solution with forced convection without symmetry planes, and the radiation heat transfer between the fin plates were not considered. Then the governing equations can be written as:

Continuity equation for 2D rectangular coordinates

$$\frac{\partial \rho}{\partial t} + \frac{\partial(\rho u)}{\partial x} + \frac{\partial(\rho v)}{\partial y} = 0 \quad (1)$$

Navier-Stokes equations for 2D rectangular coordinates

$$\rho \left(\frac{\partial u}{\partial t} + u \frac{\partial u}{\partial x} + v \frac{\partial u}{\partial y} \right) = - \frac{\partial p}{\partial x} + \mu \left(\frac{\partial^2 u}{\partial x^2} + \frac{\partial^2 u}{\partial y^2} \right) + \rho g_x \quad (2a)$$

$$\rho \left(\frac{\partial v}{\partial t} + u \frac{\partial v}{\partial x} + v \frac{\partial v}{\partial y} \right) = - \frac{\partial p}{\partial y} + \mu \left(\frac{\partial^2 v}{\partial x^2} + \frac{\partial^2 v}{\partial y^2} \right) + \rho g_y \quad (2b)$$

Energy equation for 2D rectangular coordinate

$$\rho C_p \left(\frac{\partial T}{\partial t} + u \frac{\partial T}{\partial x} + v \frac{\partial T}{\partial y} \right) = k \left(\frac{\partial^2 T}{\partial x^2} + \frac{\partial^2 T}{\partial y^2} \right) + \mu \Phi \quad (3)$$

where

$$\Phi = 2 \left[\left(\frac{\partial u}{\partial x} \right)^2 + \left(\frac{\partial v}{\partial y} \right)^2 \right] + \left(\frac{\partial v}{\partial x} + \frac{\partial u}{\partial y} \right)^2 \quad (4)$$

For natural convection, a coupled algorithm was used to solve all equations simultaneously and for forced convection an uncouple solution was used for Navier-Stokes and Energy equations. Transient regime was considered only in numerical solution for natural convection without heat sink cases. General boundary conditions for transient solutions are detailed in Tab. 4 and domain information is shown in Fig. 5a.

Table 4. Initial and boundary conditions for transient solution.

Transient solution	
Initial condition	Boundary condition
u=v=w=0 (all velocity field at rest. no initial flow)	u=v=w=0 (non slip wall)
P=0 (relative pressure specified)	u=0, v=v _{esp} (specified velocities at air inlet boundary)
T=T _{amb} (specified environment temperature)	P=0 (free boundary)
	Q=Q _{esp} (specified heat flux at extended plate)

Numerical solutions for natural convection cases without heat sink, is important to remember that the computational domain must have boundaries far enough to not interfering the region studied solution. Comunelo and Guths (2005) and Comunelo (2007) defines the computational domain for a vertical plate as approximately 180 times the plate height or 3 times the plate length. For this study the computational domain, represented in Fig. 5a, were considered H=250mm and L=250mm.

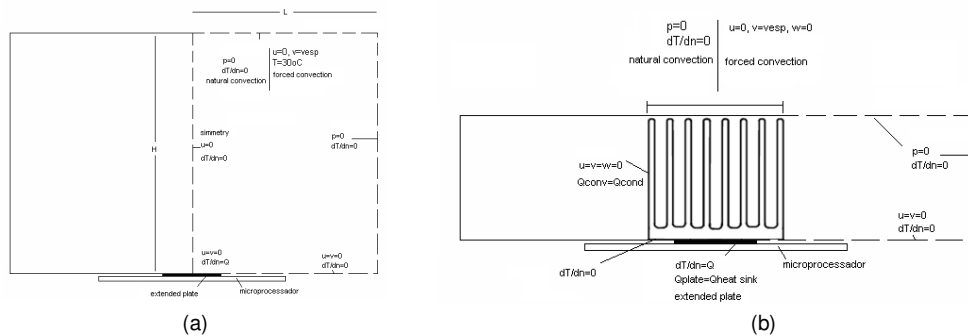


Figure 5. Numerical domain and boundary conditions: (a) without heat sink test cases, (b) with heat sink test cases.

For numerical solution, was used a software based on finite element method, Ansys[®]. General information about numerical mesh and domains are listed in Tab. 5, and mesh details are shown in Fig. 6.

Table 5. Mesh configuration.

	N _{Element}	N _{Node}	Volume [m ³]	Convective area [m ²]	L Characteristic [m]
2D mesh for natural convection					
Global	92966	94048	-	-	-
3D mesh for heat sink analysis					
Global (heat sink #1)	721927	371113	-	-	-
Solid Domain (heat sink #1)	390702	101416	1.95e-5	2.50e-2	7.81e-4
Fluid Domain (heat sink #1)	331225	327058	-	-	-
Global (heat sink #2)	618800	642360	-	-	-
Solid Domain (heat sink #2)	172200	252840	3.15e-5	4.37e-2	7.21e-4
Fluid Domain (heat sink #2)	446600	522840	-	-	-

All boundary conditions including the steady state numerical solutions are described in Tab. 6.

Table 6. Boundary conditions for numerical solutions and experimental measuring.

Case	Extended plate heat flux [W/m ²]	Inlet air velocity [m/s]	Configuration	Solution	Regime
01	10 ²	natural convection	No heat sink	numeric	transient
02	10 ²	-5	No heat sink	numeric	steady state
03	10 ²	-10	No heat sink	numeric	steady state
04	10 ³	natural convection	No heat sink	numeric	transient
05	10 ³	-5	No heat sink	numeric	steady state
06	10 ³	-10	No heat sink	numeric	steady state
07	10 ⁴	natural convection	No heat sink	numeric	transient
08	10 ⁴	-5	No heat sink	numeric	steady state
09	10 ⁴	-10	No heat sink	numeric	steady state
10	10 ⁴	-5	heat sink #1 (aluminium)	numeric	steady state
11	10 ⁴	-5	heat sink #1 (copper)	numeric	steady state
12	10 ⁵	-5	heat sink #1 (aluminium)	numeric	steady state
13	10 ⁵	-5	heat sink #1 (copper)	numeric	steady state
14	10 ⁶	-5	heat sink #1 (aluminium)	numeric	steady state
15	10 ⁶	-5	heat sink #1 (copper)	numeric	steady state
16	10 ⁴	-5	heat sink #2 (aluminium)	numeric	steady state
17	10 ⁴	-5	heat sink #2 (copper)	numeric	steady state
18	10 ⁵	-5	heat sink #2 (aluminium)	numeric	steady state
19	10 ⁵	-5	heat sink #2 (copper)	numeric	steady state
20	10 ⁶	-5	heat sink #2 (aluminium)	numeric	steady state
21	10 ⁶	-5	heat sink #2 (copper)	numeric	steady state
22	8,76x10 ⁴ (idle ref.)	natural convection	heat sink #1 (aluminium)	experiment	steady state
23	8,76x10 ⁴ (idle ref.)	natural convection	heat sink #2 (aluminium)	experiment	steady state
24	2,19x10 ⁵ (max ref.)	natural convection	heat sink #1 (aluminium)	experiment	steady state
25	2,19x10 ⁵ (max ref.)	natural convection	heat sink #2 (aluminium)	experiment	steady state
26	8,76x10 ⁴ (idle ref.)	-5	heat sink #1 (aluminium)	numeric/experiment	steady state
27	8,76x10 ⁴ (idle ref.)	-5	heat sink #2 (aluminium)	numeric/experiment	steady state
28	2,19x10 ⁵ (max ref.)	-5	heat sink #1 (aluminium)	numeric/experiment	steady state
29	2,19x10 ⁵ (max ref.)	-5	heat sink #2 (aluminium)	numeric/experiment	steady state

Intel declares that if the microprocessor is running at idle state, it dissipates 40% of maximum heat presented in Table 2.

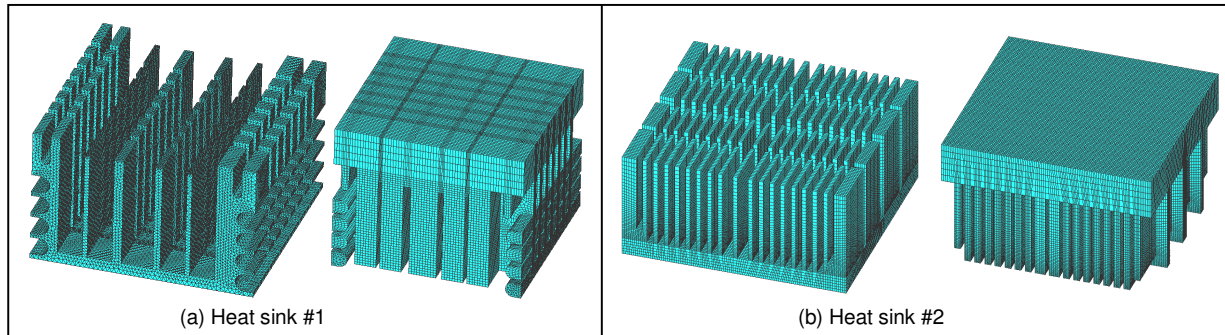


Figure 6. Numerical mesh configuration. (a) model #1, (b) model #2. Solid (left) and fluid (right) domains.

Some non dimensional groups are defined for convective heat transfer as:

$$Gr = \frac{g\beta(T_{plate} - T_{\infty})L^3}{\nu^2} \quad (\text{Grashof number}) \quad (5)$$

$$\bar{Nu}_L = \frac{\bar{h}L}{k_{ar}} = CRa_L^n \quad (\text{Nusselt number}) \quad (6)$$

$$Ra_L = Gr_L Pr = \frac{g\beta(T_{sup} - T_{\infty})L^3}{\nu\alpha} \quad (\text{Rayleigh number}) \quad (7)$$

For horizontal flat plate, Incropera and De Witt (1998) define the characteristic length as:

$$L = \frac{A_{diss}}{P} = 2,475mm \quad (8)$$

where:

A_{diss} is the convective heat transfer area.

P is the extended plate perimeter.

The mean Nusselt number is numerically evaluated for natural convection cases over the extended plate considering the configuration shown in Fig. 7, where T^* and d are non dimensional values of temperature and length.

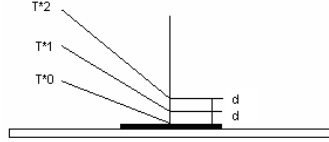


Figure 7. Temperature positions for numerical Nusselt evaluation.

The value d considered was about $0,01L$, and the non dimensional temperature was calculated as Eq. (9) and the Nusselt number was calculated as Eq. (10).

$$T^* = \frac{(T - T_\infty)}{(T_{\max} - T_\infty)} \quad (9)$$

$$Nu_{wall} = \frac{1}{2d} [-3T^*_0 + 4T^*_1 - T^*_2] \quad (10)$$

Applying the energy balance over the heat sink, not considering radiation effects and considering that the unique energy entrance is from heat sink-microprocessor contact, then the outgoing energy must be dissipated by convection through the heat sink walls to the air. Then the formulation states:

$$q_{die} = q''_{die} A_{die} = hA_{diss} \Delta \bar{T} = hA_{diss} (\bar{T}_{base} - \bar{T}_\infty) \quad (11)$$

$$h = \frac{q''_{die} A_{die}}{A_{diss} (\bar{T}_{base} - \bar{T}_\infty)} \quad (12)$$

where:

h is the heat sink global convective heat transfer coefficient.

A_{die} is the processor extended plate area.

q_{die} is the heat coming from microprocessor extended plate and is entering to the heat sink base (13)

For complex geometries, Incropera and De Witt (1998) define the characteristic length as:

$$L = \frac{Vol}{A_{HS}} \quad (14)$$

4. RESULTS

There were three classes of results: a) numerical solutions obtained by finite element modeling, b) experimental results obtained by thermocouple measurements and, c) experimental results obtained by thermographic camera measurements. For transient convection regime without heat sink, the numerical solutions for the maximum processor temperature distribution are shown in Fig. 8.

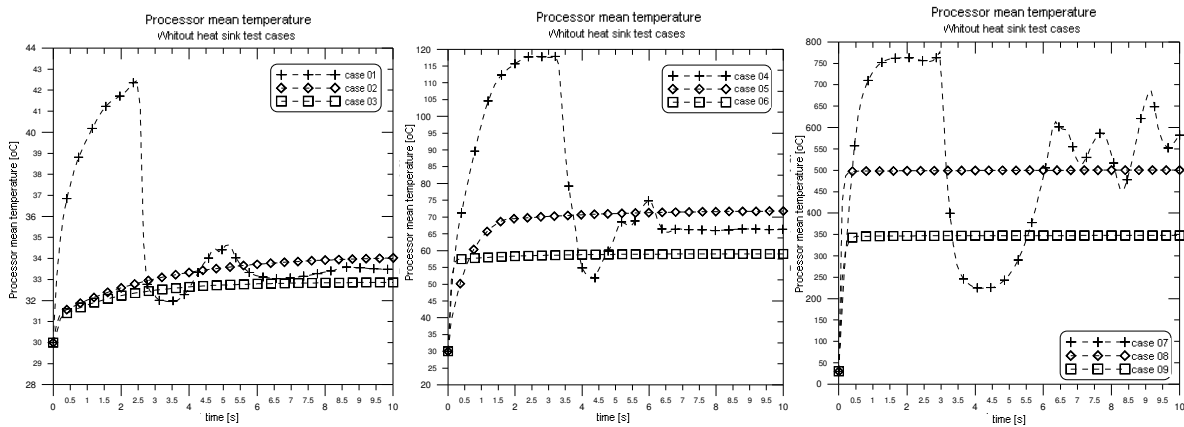


Figure 8. Microprocessor numerical transient temperature distribution – without heat sink test cases.

For test cases without heat sink, in Fig. 8 can be seen that all natural convection cases had similar behavior characterized by a very fast raise and high temperature level followed by stabilization at lower temperature. This is not seen in forced convection cases, where the temperature raises not so fast and then asymptotically reaches the steady state regime level. For 10^2 and 10^3 W/m² cases, these results have only theoretical importance because this level of power consumption is not reached in practical performance. This level is not sufficient to start the microcomputer system. The non dimensional parameters calculated for natural convection cases without heat sink are presented in Tab. 7.

Table 7. Non dimensional parameters for natural convection cases, time=10s.

Case	Ra _L (eq.7)	Gr _L (eq.5)	Nu _L (eq.10)
01	4.60	7.74	1.22
04	57.34	80.77	1.18
07	871.72	1227.77	0.79

The maximum microprocessor temperatures evaluated by numerical and experimental methods are presented in Tab. 8. This table presents the results for three different level of **cpu** usage: a) 3% of **cpu** usage as Intel® describes, represents a 40% of maximum power consumption and heat dissipation that means $8,76 \times 10^4$ W/m² b) 100% represents the maximum power consumption and heat dissipation that means $2,19 \times 10^5$ W/m² and c) BIOS represents the power level considering the system running the BIOS setup program. Specific software named HOT CPU, was used to control the **cpu** usage under Windows environment and the Windows Task Manager program was used to check the actual **cpu** usage level.

The thermocouple used was a K Type model with 0,5 °C precision, and the thermo-graphic camera used was a FLIR InfraCAM Wester model, distance from object 0,2 m and considered material emissivity 0,83 . Also was considered for experimental cases two different configurations: a) with artificial ventilation provided by a cooler and, b) without artificial ventilation.

Table 8. Maximum microprocessor temperature [°C]

Usage Level / Method	3% with cooler	3% without cooler	100% with cooler	100% without cooler	BIOS with cooler	BIOS without cooler
Thermo-graphic Heat sink #1	27.39	43.28	41.32	88.71	38.64	84.36
Experimental Heat sink #1	29	44	48	89	47	89
Numeric Heat sink #1	30.39		38.47			
Experimental Dissipador #2	30	37	48	99	46	99
Numeric Heat sink #2	32.09		42.72			

All data are for aluminium heat sink.

Using all Tab. 8 data and Eq. (6) and Eq. (12) and the nominal heat dissipation, Tab. 2, the convective heat transfer coefficient and Nusselt number can be calculated.

Table 9. h coefficient e Nusselt number

Power level	10^4 [W/m ²]		10^5 [W/m ²]		10^6 [W/m ²]		$8,76 \times 10^4$ W/m ² 3% with cooler aluminium	$8,76 \times 10^4$ W/m ² 3% without cooler aluminium	$2,19 \times 10^5$ W/m ² 100% with cooler aluminium	$2,19 \times 10^5$ W/m ² 100% without cooler aluminium
	aluminium	copper	aluminium	copper	aluminium	copper				
Method										
Experimental Heat sink #1							153.45 4.56	19.67 0.58	56.18 1.67	14.35 0.42
Numeric Heat sink #1	132.88 3.95	239.20 7.12	132.13 3.93	242.80 7.23	132.73 3.95	241.10 7.18	68.042 2.02		68.06 2.02	
Experimental Heat sink #2							42.04 1.15	17.62 0.48	22.85 0.62	7.10 0.19
Numeric Heat sink #2	31.37 0.86	36.69 1.00	29.64 0.814	36.69 1.00	29.63 0.81	36.69 1.00	29.65 0.81		29.66 0.81	

Figure 9 presents the effect of different materials in heat sink temperature distribution for reference cases 26, 27 with $8,76 \times 10^4$ W/m² (3%) of power dissipation heat sink #1 and #2, and 28, 29 cases with $2,19 \times 10^5$ W/m² (100%) of power dissipation heat sink #1 and #2.

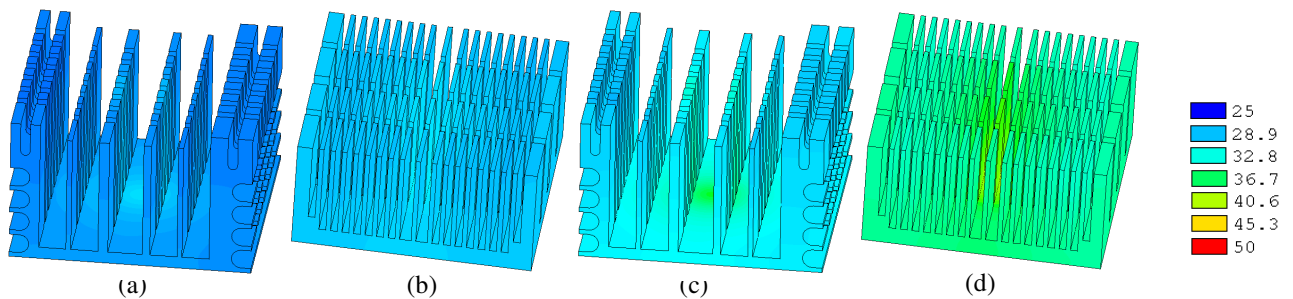


Figure 9. Heat sink superficial temperature distribution. (a) case 26, (b) case 27, (c) case 28, (d) case 29.

Figure 10 shows the temperature distribution along a symmetry line on the heat sink base.

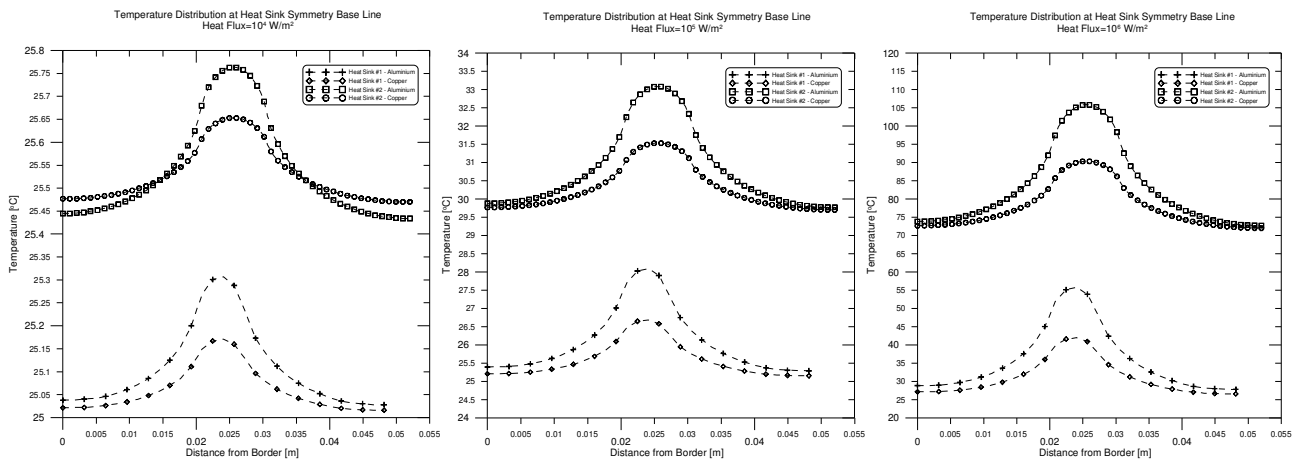


Figure 10. Numerical temperature distribution along the heat sink base

Another parameter used to estimate the heat sink-microprocessor assembly performance is defined by Intel® as the thermal resistance. This parameter can be calculated using Eq. 15 and the better performance will result in a minor parameter number. Table 10 presents the assembly performance for cases with aluminum heat sink and forced convection.

$$\theta_{JA} = \frac{(T_J - T_{amb})}{q_{die}} \tag{15}$$

where θ_{JA} : junction-ambient thermal resistance

T_J : junction temperature

T_{amb} : environment temperature

q_{die} : microprocessor heat dissipation

Table 10. Steady state regime thermal resistance

		θ_{JA} [°C/W]	
		Heat sink #1	Heat sink #2
3%	with cooler	0.31	0.36
BIOS	with cooler	1.25	1.20
100%	with cooler	1.30	1.30
3%	without cooler	1.09	0.73
BIOS	without cooler	3.45	3.97
100%	without cooler	3.45	3.97

It is known that convective heat transfer depends on fluid flow regime near wall. The Fig. 11 presents the streamlines distribution over the heat sink for forced convection cases. With this information it's possible to identify some recirculation zones and the heat sink can be redesign for better efficiency.

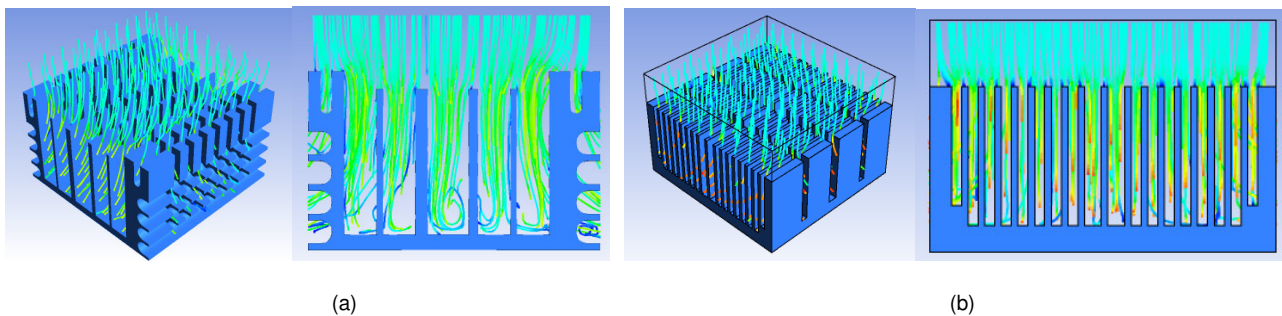


Figure 11. Streamlines. (a) heat sink #1, (b) heat sink #2.

CONCLUSION

The microprocessor temperature control is something that must be considered as priority to new products design as cooler fans and heat dissipation systems, because the use at high temperature will considerably reduce it's lifetime and raise the processing breakup.

For no heat sink natural convection cases, transient results in Fig 8, shows that the microprocessor temperature reaches prohibitive levels determined by manufacturer very fast. This means that in a case of turning on the system without any kind of heat dissipation dispositive probably the microprocessor will burnouts, if no thermal protection system is built in or if it fails. After a small time interval, the microprocessor temperature minimizes oscillation and tends to reach a steady state temperature. For forced convection cases the temperature history shows that there is no initial jump but an asymptotically tendency to a steady state level.

For heat sink cases it was possible to identify that the performance is highly dependent of constructive material, approximately 83% better for convective heat transfer coefficient and Nusselt number for copper and the maximum microprocessor temperature is around 30% lower considering the same boundary conditions.

Another important contribution for heat dissipation is the air velocity. Forced convection cases were compared to natural convection in Tab. 9, and results shows that convective coefficients heat transfer and Nusselt numbers are greater for forced convection than for natural convection, and these differences in some cases can reach over than 40% better. This behavior can be seen in Tab. 10, if compare the cases with and without cooler assembly.

The computational tool used to simulate the air flow and temperature distribution is very useful because is possible to change boundary conditions and materials to study the effect in global efficiency. For air flow over

the heat sink, Fig. 11 shows that there are some recirculation regions on base of heat sink #1, something that reduce the heat dissipation efficiency. For this case some kind of baffles could be design to eliminate the recirculation areas.

Finally, the question to be answered is: which one is the best choice. The answer will be presented since some numerical results can be evaluated. Here were presented a simple procedure to help engineers to design better heat dissipation systems, and numerical simulation shows to be a great tool to be use with experimental analysis.

REFERENCES

- Bejan, A., Jones, J. A., Krauss, A. D., 2003; "Heat Transfer Handbook", John Wiley & Sons Inc.
- Comunelo, R, Guths, S. 2005; "Natural Convection at Isothermal Vertical Plate: Neighbourhood Influence", 8p, Proceedings of COBEM 2005, 18th International Congress of Mechanical Engineering, November 6-11, Ouro Preto-MG.
- Comunelo, R. R., 2007; "Convecção Natural em Placa Plana Vertical: Influência de Superfícies Vizinhas no Coeficiente de Transferência de Calor", Dissertação de Mestrado em Engenharia Mecânica, Universidade Federal de Santa Catarina, Centro Tecnológico, Florianópolis.
- Han, Y., 2007; "Temperature Aware Techniques for Design, Simulation and Measurement in Microprocessors", Doctor Thesis, Submitted to the Graduate School of the University of Massachusetts Amherst, February.
- Incropera, F. P., De Witt, D., 1998; "Fundamentos da Transferência de Calor e de Massa", 4^a Edição, LTC Editora.
- Intel Corporation^[1], 2002; "Intel® Pentium® III Processor for the SC242 at 450 MHz to 1.0 GHz", Datasheet Document Number: 244452-009, July.
- Intel Corporation^[2], 2001; "Intel® Pentium® III Processor in the FC-PGA2 Package Thermal Design Guidelines", Order Number: 249660-001, June.
- Pecht, M., Lall, P., Hakim, E. 1992; "The Influence of Temperature on Integrated Circuit Failure Mechanisms", In *Advances in Thermal Modeling of Electronic Components and Systems*, Vol. 3, A. Bar-Cohen and A. D. Kraus, eds., ASME, New York, pp. 61–152.
- Pollack, F. J., 1999; "New Microarchitecture Challenges in the Coming Generations of CMOS Process Technologies", In Proceedings of the 32nd Annual ACM/IEEE International Symposium on Microarchitecture, Keynote Talk.
- Technology News, 2007, "Cooling Chips to -33 °C Gains a One Generation Jump in Speed", pp. 26-30, Solid State Technology, june.
- Wilcox, K., Manne, S., 1999; "Alpha Processors: A History of Power Issues and a Look to the Future", Cool Chips Tutorial, An Industrial Perspective on Low Power Processor Design in Conjunction With Micro-33, December.